Maser Polarization

Gabriele Surcis[1], Wouter H. T. Vlemmings[2], Boy Lankhaar[2] and Huib Jan van Langevelde[3,4]

[1]INAF, Osservatorio Astronomico di Cagliari
Via della Scienza 5, I-09047, Selargius, Italy
email: surcis@oa-cagliari.inaf.it

[2]Department of Space, Earth and Environment, Chalmers University of Technology
Onsala Space Observatory, 439 92 Onsala, Sweden

[3]Joint Institute for VLBI ERIC
Postbus 2, 7990 AA Dwingeloo, The Netherlands

[4]Sterrewacht Leiden, Leiden University
Postbus 9513, 2330 RA Leiden, The Netherlands

Abstract. Through the observations and the analysis of maser polarization it is possible to measure the magnetic field in several astrophysical environments (e.g., star-forming regions, evolved stars). In particular from the linearly and circularly polarized emissions we can determine the orientation and the strength of the magnetic field, respectively. In these proceedings the implications, on observed data, of the new estimation of the Landé g-factors for the CH_3OH maser are presented. Furthermore, some example of the most recent results achieved in observing the polarized maser emission from several maser species will also be reported.

Keywords. masers, polarization, magnetic fields, radiative transfer

1. Introduction

Measuring magnetic fields in the proximity of astrophysical objects, like massive young stellar objects (YSOs) or evolved stars, has always been a strong desire. This tough challenge bothered the astronomers till few decades ago when the foundations of maser polarization theory were strengthened (e.g., Nedoluha & Watson 1992). Through interferometric observations and the analysis of the polarized emission of masers it is nowadays possible both to derive the morphology and to determine the strength of magnetic field at milliarcsecond resolution, which translates for close-by objects in astronomical unit (au) scale.

The main maser species for which the polarized emission is commonly detected are OH, CH_3OH, SiO, and H_2O masers. OH is a paramagnetic molecule, i.e. the molecule has a magnetic permeability greater or equal to unity, and the splitting (ΔV_Z) due to the Zeeman effect of its masering emission lines is larger than the linewidth (Δv_L) of the maser lines themselves. The behavior of non-paramagnetic molecules (CH_3OH, SiO, and H_2O) is much less pronounced, i.e. $\Delta V_Z < \Delta v_L$. This implies that from the OH maser emissions the direct measurement of the Zeeman-splitting, and consequently of the magnetic field strength (B), is straightforward while for the other three maser species it requires a more detailed analysis. The maser emission lines arise under different physical conditions (e.g., temperatures and densities) and consequently they trace the magnetic fields in different regions of the same astronomical object. The observations and analysis of all the four maser species are therefore fundamental.

In 1992 Nedoluha & Watson developed a full radiative transfer model for the polarized emission of 22-GHz H_2O maser. The transfer equations of this model are solved in the presence of a magnetic field that causes $\Delta V_Z < \Delta v_L$, and under the following conditions:

- the Zeeman frequency shift $g\Omega$, where g is the Landé g-factor and $\Omega = eB/m_e c$, is much larger than the rate of stimulated emission R;
- the Zeeman frequency shift is much larger than the decay rate Γ and the cross-relaxation between the magnetic substates Γ_ν.

Therefore the model is valid only for unsaturated H_2O masers. Although the model was developed for the 22-GHz H_2O maser, this is valid for all the non-paramagnetic maser species that meet the above conditions. This is the case both for the CH_3OH maser emissions (Vlemmings *et al.* 2010) and for the SiO maser emissions (Peréz-Sánchez & Vlemmings 2013). However, for the SiO masers it is necessary to include the anisotropic pumping mechanism that is not considered in Nedoluha & Watson's model.

2. CH_3OH maser

CH_3OH maser emission is divided into two classes: Class I (e.g., rest frequency = 36 GHz, 44 GHz) and Class II (e.g., 6.7 GHz, 12.2 GHz). All the maser lines originate from torsion-rotation transitions and only recently an accurate model of their hyperfine structure has been calculated (Lankhaar *et al.* 2016). The model shows that each single CH_3OH maser emission is composed of several hyperfine transitions (> 8) which are not spectrally resolved due to the typical "poor" spectral resolution of the observations ($\gtrsim 2$ kHz). Indeed the frequency separations of the hyperfine transitions of a maser emission are of the order of few kHz (Tables I-XIV of Lankhaar *et al.* 2016). Actually, it is still unknown how much a hyperfine transition contributes to its maser emission, therefore a detailed pumping model is absolutely fundamental to resolve this issue.

In addition, Lankhaar *et al.* (2017) investigated the split of the hyperfine transitions when the CH_3OH molecule is immersed in a magnetic field, providing the Landé g-factor for all the transitions. Although the main results obtained from Lankhaar *et al.* can be read in this book, we just underline here that the g-factors varies with the magnetic field strength and they can be considered constant for $B \lesssim 50$ mG.

The Full Radiative Transfer Method Code

In 2010 we adapted the Full Radiative Transfer Method (FRTM) code, developed by Vlemmings *et al.* (2006) for the H_2O maser and based on the model of Nedoluha & Watson (1992), for modeling the polarized emission of the 6.7-GHz CH_3OH maser. In the FRTM code the 6.7 GHz maser emission was assumed to be composed of only one transition (no hyperfine structure was considered), and later the assumed g-factor value was found to be innacurate (Vlemmings et sl. 2011). Note that the fact that the g-factor and the hyperfine structure are unknown does not influence the analysis of the linearly polarized emission, from which is possible to determine the emerging brightness temperature ($T_b\Delta\Omega$) and the intrinsic thermal linewidth (ΔV_i) of the maser line, and the θ angle (the angle between B and the maser propagation direction). On the contrary, the measurement of the Zeeman-splitting and the estimates of the magnetic field strength strongly depend on both the hyperfine structure and the g-factors. For this reason no magnetic field strength measured from the circularly polarized emission of CH_3OH maser has been provided (e.g., Surcis *et al.* 2015). Thanks to the work of Lankhaar *et al.* (2017) we were able to modify the FRTM code in order to model properly not only the polarized emission of the

6.7 GHz CH_3OH maser, but the polarized emission of all the torsion-rotation transitions. We assumed that eight hyperfine transitions contribute equally to each CH_3OH maser emission (see Lankhaar *et al.* in this book), with the g-factors and Einstein coefficients as tabled in Lankhaar *et al.* (2017). We also assumed that $B = 10$ mG and that the temperature of the incoming radiation is 25 K. Furthermore, we have implemented a new subroutine for calculating the Clebsch-Gordan coefficients.

Theoretical results

We have run the code, so far, for three of the CH_3OH maser emissions: 6.7 GHz, 36 GHz, and 44 GHz. Part of the results are plotted in Fig. 1. We run the code considering a linewidth of the maser (Δv_L) of 0.2 km s^{-1} and an intrinsic thermal linewidth (ΔV_i) of 1.0 km s^{-1}.

For the 6.7-GHz maser transition (Class II) the rebroadening of the maser line, i.e. when the maser is entering the saturation state, happens when $T_b \Delta\Omega = 10^9 - 10^{10}$ K sr and consequently the expected linear polarization fraction for unsaturated maser is $P_L \lesssim 5\%$. If we assume that there exists one hyperfine transition dominating the maser emission, for instance that one with the largest Einstein coefficient for stimulated emission (A; Lankhaar *et al.* this book), we obtain similar results for P_L but the expected circular polarization fraction (P_V) increases considerably. The upper limit changes from $P_V < 0.2\%$ to $P_V < 0.7\%$, the letter matching the observations.

For the 36-GHz and 44-GHz maser transitions (Class I) the rebroadening is observed at lower brightness temperature than for the 6.7-GHz transition. The model predicts that this happens for $T_b \Delta\Omega = 5 \cdot 10^7 - 5 \cdot 10^8$ K sr and $T_b \Delta\Omega = 10^7 - 10^8$ K sr for the 36-GHz and the 44-GHz, respectively. Consequently for unsaturated masers we have $P_L^{36GHz} \lesssim 7\%$ and $P_L^{44GHz} \lesssim 4\%$. The upper limit of P_V increases, for both 36-GHz and 44-GHz maser emission, from a fraction of *per thousands* to fraction of *percent* if the hyperfine transition with the largest A coefficient is considered.

The Flux-Limited sample

Since 2008 we have observed 30 massive star-forming regions to detect the polarized emission of 6.7-GHz CH_3OH masers (the so-called Flux-Limited sample), 25 of which have been already analyzed and partially published (e.g., Surcis *et al.* 2015 and references therein). Most of the maser features were modeled by using the old FRTM code and so at the time of the pubblications no magnetic field strength was estimated due to the uncertainty of the g-factor. Thus we modeled again the maser features by using the new version of the code described above and for which the hyperfine transition F = 3 $\longrightarrow$ 4 is assumed to dominate the maser emission (see Lankhaar *et al.* this book). We found that the obtained values of $T_b \Delta\Omega$, ΔV_i, and θ are the same within 1% to the previously measured ones and that the magnetic field strength ranges between 1 mG and 15 mG. Only in the case of NGC 7538 the magnetic field is particularly strong, $B \lesssim 50$ mG, needing a closer investigation with further observations.

3. SiO maser - the case of VY CMa

Since the last maser symposium in Stellenbosch (South Africa) several results have been achieved in observing the polarized emission of SiO masers (e.g., Assaf *et al.* 2013, Richter *et al.* 2016). One of the most recent results is the detection of the polarized emission of the SiO masers for the first time with the Atacama Large Millimeter/submillimeter Array (ALMA) around the red supergiant VY CMa (Vlemmings *et al.* 2017). Using Band 5 of ALMA they detected varying levels of P_L for ^{28}SiO (J=4-3, ν=0,1,2)
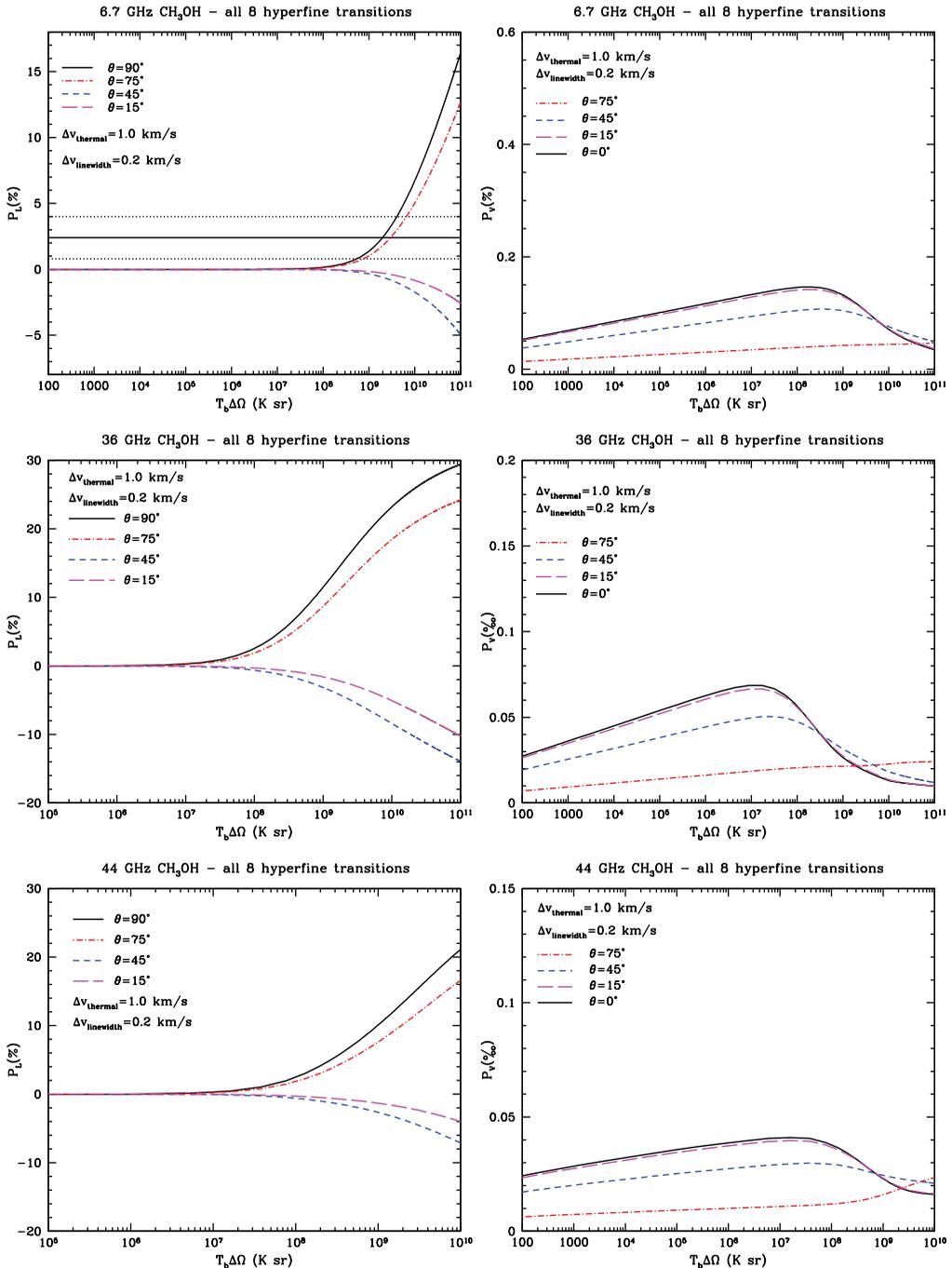
Figure 1. Outputs of the FRTM code for the 6.7 GHz, 36 GHz, and 44 GHz CH₃OH maser emissions. The plots are obtained by assuming that all the eight hyperfine transitions, which are listed in Lankhaar *et al.* (2017), contribute equally to the maser emission. Left panels: the fractional linear polarization vs. the emerging brightness temperature. The horizontal black dashed lines indicate the range of typical P_l measured towards 6.7 GHz CH₃OH masers. Right panels: the fractional circular polarization vs. the emerging brightness temperature.
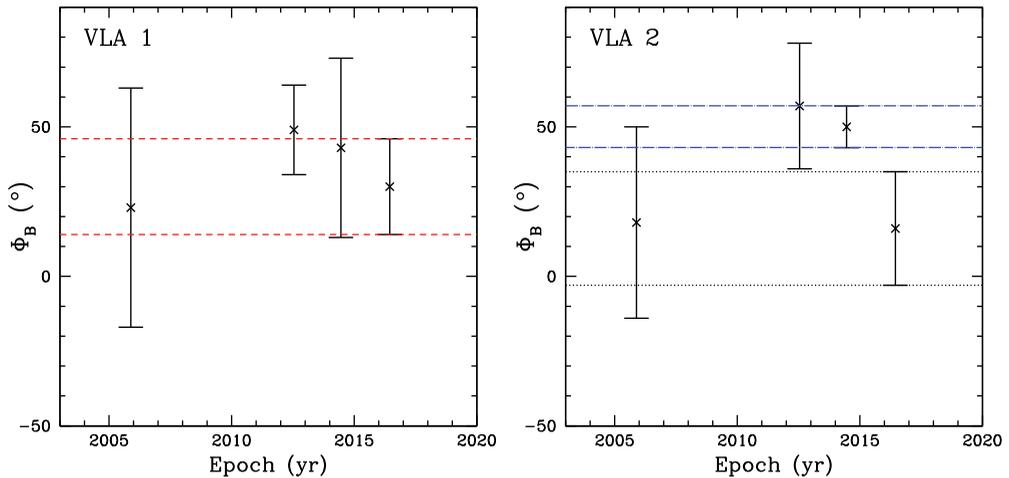
Figure 2. Multi-epoch comparison of magnetic field angles (Φ_B) for the massive YSOs VLA 1 (left panel) and VLA 2 (right panel) in W75N(B). The red dashed lines indicate the common range of angles among the four epochs (2005.89, 2012.54, 2014.46, and 2016.45). The black dotted lines indicate the common range of angles between epochs 2005.89 and 2016.46, and the blue dash-dotted ones between epochs 2012.54 and 2014.46.

and ^{29}SiO (J=4-3, ν=0,1) maser lines (rest frequency $\sim$ 170 GHz). In particular they observed a clear structure in the PA of the linear polarization vectors of ^{28}SiO (J=4-3, ν=1) similar to that observed by Herpin *et al.* (2006) at 86 GHz. The vectors rotate from $\sim$130° at blue-shifted velocities to $\sim$ −50° around the stellar velocity and back to $\sim$140° on the red-shifted side, suggesting the presence of a possible complex toroidal magnetic field morphology (Vlemmings *et al.* 2017).

4. H$_2$O maser - the case of W75N(B)

From 1999 to 2012 we have monitored the expansion of a 22-GHz H$_2$O maser shell around an unresolved continuum source excited by the massive YSO W75N-VLA2 with VLBI observations. We found that this shell is expanding at about 5 mas/yr and, more importantly, that it has evolved from an almost circular wind-driven shell to an elliptical morphology (see also Kim *et al.* this book). This suggests that we are observing in "real time" the transition from a non-collimated outflow event into a collimated outflow/jet structure during the first stages of evolution of a massive YSO. Moreover we have measured the magnetic field in two epochs separated by 7 years (in 2005 and in 2012). In this time interval the magnetic field changed its orientation following the rotation of the major-axis of the elliptical structure and decreases its strength. At 1200 au NW a more evolved YSO, named VLA 1, shows immutable H$_2$O maser distribution and magnetic field morphology. The presence of this nearby source reinforces the results of VLA 2 (Surcis *et al.* 2014).

In 2014 we started an European VLBI Network (EVN) monitoring project (four epochs separated by two years from one another) with the aim to follow both the expansion of the outflow/jet structure in VLA 2 and, more importantly, the variation of the magnetic field in the region. The first two epochs were observed in 2014 and 2016.

While the magnetic field around VLA 1 is still the same over time, with only an increment of the magnetic field strength of the order of 2.5 times, the magnetic field around VLA 2 changed again (Fig.2). In 2014 it was perfectly in agreement with the orientation

measured in 2012, while in 2016 the magnetic field rotated back to its 2005 orientation (Fig.2). With respect to the conclusions of Surcis *et al.* (2014), who stated that the magnetic field around VLA 2 changed its orientation according to the new direction of the major-axis of the shell-like structure, this is unexpected. The next two EVN epochs (2018 and 2020) will hopefully help to clarify the phenomenon. In 2016 we also measured a magnetic field around VLA 2 15 times stronger than what was measured in 2012 by Surcis *et al.* (2014). This could be due to a further compression of the gas at the shock front caused by the encounter with a much denser medium than in the past, suggested also by the flaring of the H_2O maser features and to the stop of the maser expansion. More details of the recently achieved results could be read in Surcis *et al.* (*in prep.*).

5. The Future

The detection of polarized emission from several maser species is common nowadays. Besides the snapshots presented here there have been more interesting results that are highlighted in this book, both as talk contributions and as poster contributions. Although some scientific wishes that were expressed in 2012 in Stellenbosch (South Africa, IAUS 287) have been realized, like the determination of g-factors for CH_3OH maser emission or maser polarization observations with ALMA, many issues are still open or just popped up. Among these we would like to focus the attention on some of them:

• model the pumping mechanisms for Class I and Class II CH_3OH masers in order to determine the contributions of each single hyperfine transitions to the observed maser lines;

• confirm observationally the theoretical predictions made by the FRTM code;

• modify the FRTM code in order to include the anisotropic pumping mechanism of the SiO masers.

A bright future for maser polarization is beginning and the improvement of existing facilities and the construction of new facilities will help to make it even brighter.

References

Assaf, K. A., Diamond, P. J., Richards, A. M. S., & Gray, M. D. 2013, *MNRAS*, 431, 1077

Herpin, F., Baudry, A., Thum, C., Morris, D., & Wiesemeyer, H. 2006, *A&A*, 450, 667

Lankhaar, B., Groenenboom, G., & van der Avoird, A. 2016, *J. Chem. Phys.*, 145, 24

Lankhaar, B., Vlemmings, W. H. T., Surcis, G., van Langevelde, H. J., Groenenboom, G., & van der Avoird, A. 2017, *Nature Astronomy*, 2, 145L

Nedoluha, G. E. & Watson, W. D. 1992, *ApJ*, 384, 185

Peréz-Sánchez, A. F. & Vlemmings, W. H. T. 2013, *A&A*, 551A, 15

Richter, L., Kemball, A., & Jonas, J. 2016, *MNRAS*, 461, 2309

Surcis, G., Vlemmings, W. H. T., van Langevelde, H. J., Goddi, C., Torrelles, J. M., Cantó, J., Curiel, S., Kim, S.-W., & Kim, J.-S. 2014, *A&A*, 565, L8

Surcis, G., Vlemmings, W. H. T., van Langevelde, H. J., Hutawarakorn Kramer, B., Bartkiewicz, A., & Blasi, M. G. 2015, *A&A*, 578, 102

Vlemmings, W. H. T., Diamond, P. J., van Langevelde, H. J., & Torrelles, J. M. 2006, *A&A*, 448, 597

Vlemmings, W. H. T., Surcis, G., Torstensson, K. J. E., & van Langevelde, H. J. 2010, *MNRAS*, 404, 134

Vlemmings, W. H. T., Torres, R. M., & Dodson, R. 2011, *A&A*, 529, 95

Vlemmings, W. H. T., Khouri, T., Martí-Vidal, I., Tafoya, D., Baudry, A., Etoka, S., Humphreys, E. M. L., Jones, T. J., Kemball, A., O'Gorman, E., Peréz-Sánchez, A. F., & Richards, A. 2017, *A&A*, 603, 92